A pediatric quantitative systems pharmacology model of neurofilament trafficking in spinal muscular atrophy treated with the antisense oligonucleotide nusinersen

Alessio Paris[1] | **Pranami Bora**[1] | **Silvia Parolo**[1] | **Drew MacCannell**[2] | **Michael Monine**[2] | **Nick van der Munnik**[2] | **Xiao Tong**[2] | **Satish Eraly**[2] | **Zdenek Berger**[2] | **Danielle Graham**[2] | **Toby Ferguson**[2] | **Enrico Domenici**[1,3] | **Ivan Nestorov**[2] | **Luca Marchetti**[1,3]

[1]Fondazione The Microsoft Research - University of Trento Centre for Computational and Systems Biology (COSBI), Rovereto, Italy

[2]Biogen, Inc., Cambridge, Massachusetts, USA

[3]Department of Cellular, Computational and Integrative Biology (CIBIO), University of Trento, Trento, Italy

Correspondence
Luca Marchetti, Fondazione The Microsoft Research - University of Trento Centre for Computational and Systems Biology (COSBI), Rovereto, Italy and Department of Cellular, Computational and Integrative Biology (CIBIO), University of Trento, Trento, Italy.
Email: marchetti@cosbi.eu; luca.marchetti@unitn.it

Present address
Drew MacCannell, Dyne Therapeutics, Waltham, Massachusetts, USA

Nick van der Munnik, GSK, Greater Boston, Massachusetts, USA

Satish Eraly, Alnylam Pharmaceuticals, Cambridge, Massachusetts, USA

Abstract

Phosphorylated neurofilament heavy subunit (pNfH) has been recently identified as a promising biomarker of disease onset and treatment efficacy in spinal muscular atrophy (SMA). This study introduces a quantitative systems pharmacology model representing the SMA pediatric scenario in the age range of 0–20 years with and without treatment with the antisense oligonucleotide nusinersen. Physiological changes typical of the pediatric age and the contribution of SMA and its treatment to the peripheral pNfH levels were included in the model by extending the equations of a previously developed mathematical model describing the neurofilament trafficking in healthy adults. All model parameters were estimated by fitting data from clinical trials that enrolled SMA patients treated with nusinersen. The data from the control group of the study was employed to build an in silico population of untreated subjects, and the parameters related to the treatment were estimated by fitting individual pNfH time series of SMA patients followed during the treatment. The final model reproduces well the pNfH levels in the presence of SMA in both the treated and untreated conditions. The results were validated by comparing model predictions with the data obtained from an additional cohort of SMA patients. The reported good predictive model performance makes it a valuable tool for investigating pNfH as a biomarker of disease progression and treatment response in SMA and for the in silico evaluation of novel treatment protocols.

Study Highlights

WHAT IS THE CURRENT KNOWLEDGE ON THE TOPIC?
It was demonstrated that high levels of phosphorylated neurofilament heavy subunit (pNfH) in cerebrospinal fluid and blood are a biomarker of disease onset in

spinal muscular atrophy (SMA) and that they are reduced when SMA patients are treated with nusinersen.

WHAT QUESTION DID THIS STUDY ADDRESS?
Is it possible to build a mathematical model that describes the trafficking of pNfH in untreated and treated SMA pediatric patients?

WHAT DOES THIS STUDY ADD TO OUR KNOWLEDGE?
We extended a previously developed mathematical model in adult healthy subjects to describe the pNfH trafficking in pediatric SMA patients. The model was parametrized on clinical data and demonstrated good predictive performance in reproducing the change of pNfH levels in SMA patients at different ages, except in newborns, and during nusinersen administration.

HOW MIGHT THIS CHANGE DRUG DISCOVERY, DEVELOPMENT, AND/OR THERAPEUTICS?
The performance of the model makes it a valuable tool for investigating pNfH as a biomarker of disease severity and treatment response in SMA and for in silico evaluation of novel treatment protocols.

INTRODUCTION

Spinal muscular atrophy (SMA) is a rare, genetic progressive neurodegenerative disease characterized by a loss of motor neurons and consequent muscular weakness.[1,2] It can manifest in all stages of life, leading to different SMA types with different severities, and it is most impactful in types featuring onset in pediatric ages, with high severity and lethality, especially in children younger than the age of 2 years.

SMA is predominantly caused by homozygous deletions in the *SMN1* gene, which encodes the survival motor neuron (SMN) protein.[3,4] The *SMN1* genomic region harbors an almost identical copy of the gene, termed *SMN2*, which is responsible for a small amount of SMN protein production. Nusinersen (commercialized by Biogen, Cambridge, MA, USA as Spinraza) is an antisense oligonucleotide (ASO) approved for SMA treatment that increases the level of SMN protein by promoting the expression of full-length *SMN2* transcripts.

In SMA, as in other neurogenerative diseases, it is of compelling importance the identification of efficient and noninvasive biomarkers to monitor the progress of the disease and treatment efficacy. Neurofilament (Nf) proteins, and in particular the light and phosphorylated heavy (pNfH) isoforms, have been investigated as potential biomarkers for several neurodegenerative disorders characterized by axonal degeneration.[5–7] When released from neurons because of axonal damage, Nfs can be detected in cerebrospinal fluid (CSF) and blood. Peripheral pNfH concentrations in patients affected by several neurological diseases, including SMA,[8] are significantly higher than in healthy subjects. pNfH was also identified as a disease-sensitive pharmacodynamic response biomarker in SMA

after the observation of concentration reduction in CSF and plasma following treatment with nusinersen.[8,9]

In a previous article, we presented a mathematical model of Nf transport in healthy subjects in the age range of 20–90 years.[10] The aim of this work is to update and extend the model to provide a quantitative systems pharmacology model describing the pNfH trafficking in the SMA condition in the untreated and treated conditions during pediatric ages (0–20 years). We considered the physiological changes typical of the pediatric age that could affect Nf concentrations, in particular the differential growth of the tissue volumes and the peculiar development of the central nervous system (CNS). The impact of SMA and the effect of treatment were included by adding additional reactions to the model while parameter estimates were computed by fitting clinical data.

METHODS

Experimental data

The development and the parameterization of the model were mainly based on pNfH data in the CSF and plasma collected during the SHINE open-label extension trial[11] and during the studies NURTURE,[12] EMBRACE,[13] ENDEAR,[8,14] and CHERISH.[15] A group of 98 healthy pediatric subjects from ENDEAR[14] was preliminarily considered to perform a reparameterization of the healthy adult model[10] and validate the new assumptions relative to the healthy pediatric scenario independently from the successive assumptions included to model SMA. A total of 359 SMA patients was considered for the model parameterization of the SMA untreated scenario. They include a

control group of 17 patients who did not receive any treatment, a second group who received the treatment only in the second phase of the trial, and a group of patients to whom nusinersen was administered from the beginning. For most treated patients, data from both CSF and plasma were available, but for 30 individuals only data in plasma were collected (see Table S1 regarding the contribution of each study to the total number of subjects considered in this work). The control group measurements, together with all other pNfH measurements taken before the drug administration (i.e., at screening for those who were treated from the beginning or in the first part of the trial for those who received the treatment later) were considered to parametrize an untreated version of the model.

The patients who received the treatment were divided into two groups. A group of 278 patients was considered for the training of the treatment model. We excluded from this group patients with only pNfH data in plasma and the group of 24 patients aged younger than 3 months from the NURTURE study[12] for reasons that will be explained. A group composed of 25 patients (approximately 10% of the data set size) was employed to validate the model, whereas all remaining patients were used to train the model by fitting individual time series and compute a set of digital twins of the considered patients. The patients included in the validation set were further divided into four subgroups to obtain subject validation cohorts with homogeneous age

and treatment dosages. Two of these subgroups included patients who only had plasma data collected. Information about the treatment protocols employed for model validation are reported in Table S2.

Drug administration was different among the patients and presents several differences both in the dosage (from 1 to 12.5 mg with different doses sometimes administered to the same patient) and in the timing of the administrations. pNfH data sampling was heterogeneous as well, and in some cases pNfH data collection started only after the treatment start. The age of the enrolled patients ranged from birth up to 22 years.

Mathematical model

The starting point for the mathematical implementation of the model in the pediatric age is a previous ordinary differential equation (ODE) model for Nf trafficking in healthy adults,[10] to which we refer for an introductory overview of the details of the model. The updated diagram representing the extension to SMA is illustrated in Figure 1. The original model includes all Nf subunits, but in this work we focused only on pNfH because of its relevance to SMA[8] and data availability.

The first model extension was to include the effect of the volume growth of the tissues considered in the model
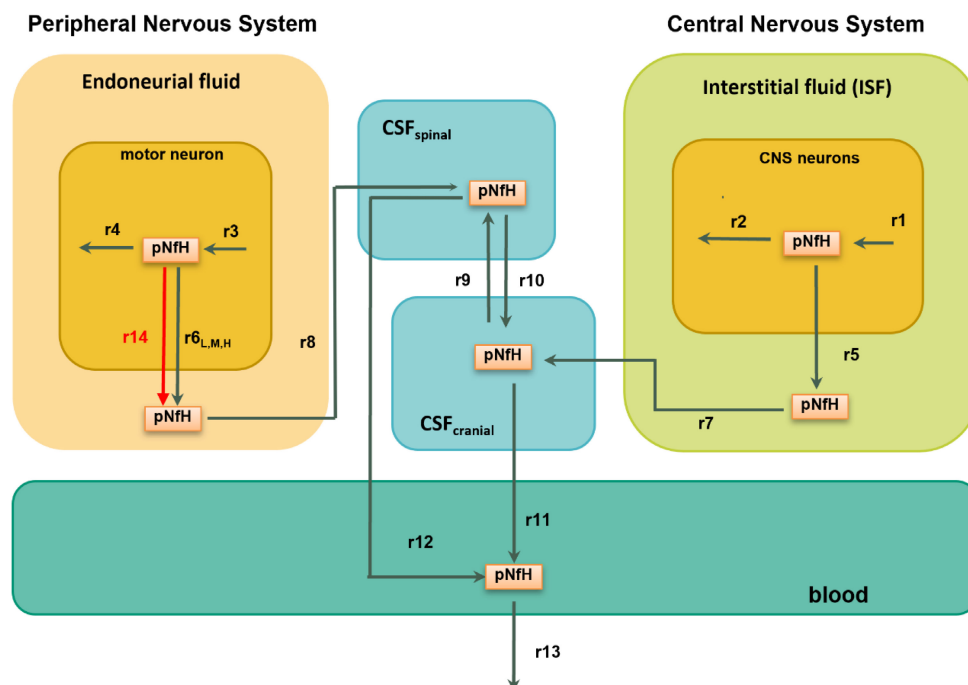

FIGURE 1 Model diagram representing the structure of the neurofilament (Nf) trafficking model. Nf subunits move from neurons to the cerebrospinal fluid and to the blood, where they are detected. The additional reaction r14 representing the additional contribution to the pNfH leakage from the peripheral nervous system caused by spinal muscular atrophy is depicted in red. CNS, central nervous system; CSF, cerebrospinal fluid; pNfH, phosphorylated neurofilament heavy subunit

in the age range of 0–20 years. The growth rates of the different compartments are different, and this can have a significant impact on the Nf concentrations given that they depend on the compartment volumes by definition. To reproduce the development in children in a realistic way, we combined information from different sources. For CNS, interstitial fluid (ISF) and blood, we combined equations relating tissue volumes to body parameters (weight, height, body mass index) obtained by fitting population data[16] with data relating the median body parameters to age.[17] Then, we assumed the change in peripheral nervous system (PNS) and endoneurial fluid volumes to be proportional to the median body height.[17] Finally, CSF cranial and spinal volumes were determined by an empirical function of age across the pediatric population, as was introduced previously[18] (see Formulas S1–S7 and Table S3 for selected volume values and references). The mathematical justification for this addition is reported in Appendix S1. Following this approach, we obtained volume growth curves as a function of age (Figure S1), and we replaced fixed volume values in the pNfH ODEs with time-dependent values. An additional term, proportional to the derivative of the volume, has been also added to the right-hand side of each pNfH ODE (Equations S9–S15).

A second factor requiring model extension was the need of reproducing the development of the CNS. The process of synaptogenesis starts during gestation and continues in the postnatal years, stopping between 2 and 5 years after birth. It is followed by a period of synapse and dendrite elimination known as pruning, lasting until the age of 10–15 years.[19] During the synaptic pruning, up to 60% of neuronal connections are eliminated, thus we expect that this process affects Nf concentration in the CNS and the Nf leakage rate. Lacking any direct measurement of this correlation, we decided to model it through phenomenological formulas[20] describing the neuronal development and by optimizing their parameters to match healthy subject Nf concentrations in the CNS (see Formulas S16–S18). We modified the synthesis rate r1 and the leakage rate r5 according to age-dependent functions as reported in Appendix S1.

The contribution of SMA to pNfH trafficking was included with an additional reaction added to the model (r14 in the diagram of Figure 1), representing the additional leakage from the PNS attributed to the disease. We assigned it a rate under the form

$$r14 = r14_A + r14_B \times r14_C^{-age} \tag{1}$$

where the last term is explicitly dependent on age. The choice of this form will be justified a posteriori by the fit of the data of the untreated patients. Figure S2 reports a plot of r14 and of the two terms composing the rate as in Equation (1).

The major target of treatment with nusinersen is the spinal cord motor neurons, and it is accounted for with the inclusion of a previously published semimechanistic physiological-based pharmacokinetic (PBPK) model[18] describing the time-dependent distribution of intrathecally administered nusinersen in the CSF, plasma, spinal cord, and several brain regions. It was originally developed based on the preclinical nusinersen study data in nonhuman primates (NHPs) and was further translated to pediatrics by applying allometric relationships to scale the rate constants. The reduction of the Nf concentration is an indirect effect of the action of the ASO. For this reason, the effect of nusinersen was modeled by multiplying the reaction r14 by a factor proportional to an effective time-dependent drug profile, determined as the output of a transit compartment model.[21] This part of the model comprises a diffusion chain through three virtual compartments (Figure S4), whose input is the ASO amount time series in the spinal cord computed for each subject according to the PBPK model of Biliouris et al.[18] The time series is computed for each patient according to the individual administration protocol followed in the trial. The ODEs of the transit compartment model are reported in Equations S20–S24.

The pNfH model is implemented as a collection of R scripts, and it is provided in Appendix S2. The R libraries *deSolve* and *optim* were used for ODE integration and optimization, respectively. All optimizations use the least-squares algorithm normalized to the absolute data values, apart from the generation of the SMA untreated population, for which an optimization with a modified target function was used as explained later. For the integration, the *lsoda* method with the default relative tolerance of 10^{-6} was used, whereas the optimization was performed using the Nelder–Mead method with the default relative tolerance of 10^{-8}.

RESULTS

As a preliminary step for the successive SMA analysis, reaction rates r5, r6, and r13, previously estimated in the original mathematical model on adult data from the literature,[10] were reestimated on pediatric healthy data. The aim of this fit is to test the validity of the assumptions related to the physiology of the pediatric age (volume growth and CNS development). We report the plots comparing the simulated time series to the data in Figure 2 (orange dashed line). In CSF, we observe a good agreement of the simulated concentrations, especially in the age range of 0–7 years. In blood, the simulation fits reasonably well in the whole selected range. The only case
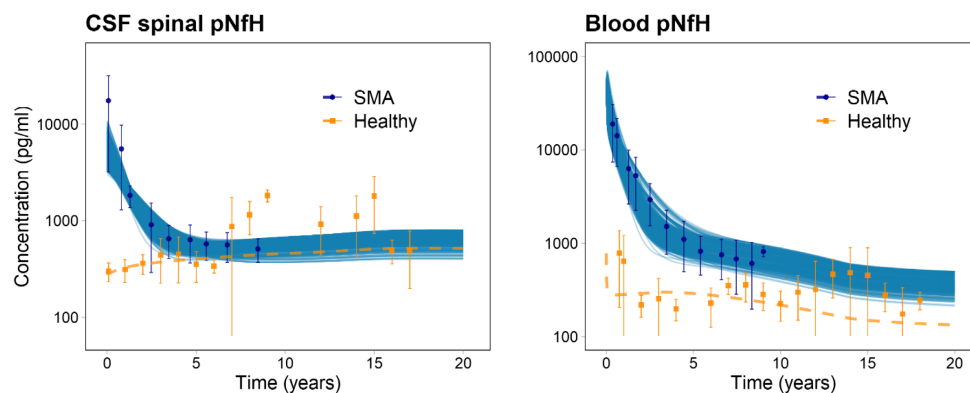
FIGURE 2 Simulated pNfH concentration time series in CSF spinal (left) and blood (right) in the healthy condition (dashed orange line) and in the in silico untreated population (continuous blue lines) compared with the corresponding healthy (orange squares and error bars) and SMA (blue circles and error bars) data. Table S6 reports the initial pNfH concentrations at birth in all compartments for the healthy condition and for an average SMA scenario. CSF, cerebrospinal fluid; pNfH, phosphorylated neurofilament heavy subunit; SMA, spinal muscular atrophy

where the fit is not optimal is in the very first months, where the higher pNfH levels are not well captured by the computed curve that decreases much faster than the measured concentration. This could be related to the hypotheses included in the model to represent the pediatric case, which may be not completely satisfied in the first 3 months of life, as detailed in the Discussion. Novel estimated rate values are compared with those computed in the original adult healthy model[10] in Table S5. Although we observed similar values for the rates r5 and r6, a relevant difference is observed in the rate of pNfH clearance in blood, where the new value of the rate is 0.33 day^{-1}, whereas the average value reported in Paris et al.[10] is 7.4 day^{-1} ([1.1, 20.1] as 95% confidence interval [CI]). We think that this discrepancy is unrelated to the pediatric physiology, but it is probably a consequence of the different immunoassays used to measure the plasma pNfH in the cohort used for the model parameterization. The immunoassays employed to obtain the data used in this work return significantly higher pNfH levels than other assays,[8,22] which are reflected in a lower estimated clearance rate in blood than that originally estimated in the healthy adult model.[10]

To parametrize the SMA model, we built a virtual population of 400 subjects compatible with the data from the untreated condition using a method recently reported in literature[23] (see Appendix S1 for further details). Each subject of the population is obtained by estimating a set of four rate values, which includes the three parameters composing r14, representing the additional contribution of SMA to the pNfH trafficking and the clearance of pNfH in blood r13. We fixed the leakage rates r5 and r6 to the values obtained from the healthy optimization, but we included the blood clearance rate r13 in the optimization set to leave an additional degree of freedom for the fits. We

then checked if the optimized rate values were consistent with the healthy parameterization. Figure 2 reports the time series we obtained for the in silico untreated population and the data used to generate them (blue lines and circles). The good agreement between the simulation and the data confirms the suitability of the formula employed to represent the SMA contribution in r14. The only part where the simulated population seems to provide a suboptimal fit of the data is in the very first months in CSF, where the population covers only the lower part of the measured pNfH intervals. As previously anticipated, we think that this indicates a possible limitation of the model in reproducing the neonatal period. Potential improvements to the model to increase the simulation accuracy in the corresponding age range are presented later. Table 1 reports the distributions of the computed parameter estimates.

The SMA-treated condition was determined through individual fits of the CSF and plasma measured time series and the estimation of six parameters of the model relying on normalized least-squares optimizations. Two of the parameters, EC50 and k_{diff}, representing the half maximal effective concentration and the diffusion rate of the drug through the transit model compartments, respectively (see Equations S20–S24) are left unconstrained in the optimization. On the other side, we refined the estimates of the three parameters composing r14 and of the blood clearance rate r13 by constraining their optimization to the estimate ranges previously determined by fitting the untreated population data. This choice was dictated by the fact that the data collection for some patients started later than the start of the treatment, and this prevents a reliable determination of the initial pNfH concentrations. In Figure 3, we show an example of the results of the individual fits, randomly chosen as representative of the accuracy

TABLE 1 Estimated model parameters computed from the generated untreated population and from the fit of the individual time series of treated patients (the full list of model parameters is provided in Table S4)

Parameter	Estimate computed from the untreated virtual population	Estimate computed from the individual treatment fits
r14$_A$ (1/day)	$(1.6 \pm 1.0) \times 10^{-7}$	$(1.04 \pm 1.72) \times 10^{-7}$
r14$_B$ (1/day)	$(1.8 \pm 0.6) \times 10^{-5}$	$(1.56 \pm 1.0) \times 10^{-5}$
r14$_C$	3.3 ± 0.9	3.25 ± 0.12
r13 (1/day)	0.10 ± 0.01	0.12 ± 0.03
EC50 (ng/ml)	-	$(5.5 \pm 2.1) \times 10^{2}$
k_{diff} (1/day)	-	0.09 ± 0.08

Abbreviations: EC50, half maximal effective concentration; k_{diff}, diffusion rate of the drug.

of the fit among all the large number of individual plots. The plots show good agreement between the model simulation and data.

To assess the global accuracy of the computed individual fits, we computed the root mean square deviation (RMSD) of the fitted time series for each patient. Figure 4 shows the results in a couple of histograms for the CSF and blood compartments. Most of the RMSDs are concentrated toward lower values (median values 113 pg/ml in CSF and 528 pg/ml in blood), confirming the general validity of the individual fits and their reliability in acting as digital twins of the considered patients. The long right-side tails of the histograms represent a smaller number of cases where the predictions are less accurate. In general, the largest deviations in absolute terms come from the measurements taken in patients aged younger than 2 years, and this explains why in absolute terms the median RMSD in plasma is higher than in CSF. In fact, plasma measurements were collected more frequently than in CSF at younger ages, when the pNfH levels in general are higher and the deviations are potentially higher in absolute terms as well. To confirm this interpretation, we also computed a normalized RMSD (NRMSD), where the normalization is computed at each point according to the following formula:

$$\text{NRMSD} = 100 \times \sqrt{\sum_{t=1}^{N} \frac{\left(y_t^{\text{pred}} - y_t\right)^2}{y_t^2} / N} \qquad (2)$$

where y_t and y_t^{pred} are the experimental and the simulated concentrations computed at the time corresponding to the data collection, respectively, and N is the total number of points in the individual time series. From the NRMSD histograms of Figure 4, we see that the results in the two compartments are similar, confirming that the fits have similar accuracy expressed in relative terms (median values 50% in CSF and 60% in blood).

Table 1 reports the distribution of the parameters of the untreated population and of the individual treatment fits. The fact that the ranges of all the parameters

are consistent between the two optimizations is expected because the individual fits were constrained by the results of the untreated population. In general, parameter estimates from the individual treatment fits reflect a larger variability in the fitted initial pNfH levels. Considering the passage through the virtual compartments, the average estimate 0.09 1/day for k_{diff} corresponds to an average time delay of approximately 40 days between the maximum of the input function and that of the effective function acting on the SMA leakage. This gives a rough estimate of the delay expected between the drug administration and the effect on the biomarker.

Model validation has been computed for 25 treated patients (approximately 10% of the data set size), which have been further divided into four validation groups to obtain cohorts with homogeneous ages and treatment dosages as detailed in the Methods and in Table S2. For each validation group, a set of 300 simulated treatment time series has been generated by model simulation according to the parameter distributions gathered from the individual fits. The sample was then refined to have the mean of the time series matching the average initial measured concentration for each validation group. Finally, a random resampling technique was applied to estimate the mean and the corresponding 95% CI of in silico samples with the same size of their corresponding real patients' samples. The results are graphically compared with the measured time series in Figure 5, where a substantial agreement of the model prediction (blue area) with the measured time series (gray points and broken lines) can be appreciated.

DISCUSSION

The extension of a previously developed Nf trafficking model in healthy adults[10] to the pediatric scenario required several modifications before including the reactions representing the effect of SMA. Drug modeling in children, in particular estimating organ volumes, often resorts to approximate but effective methods such as allometric scaling.[24] In this work, we moved in the
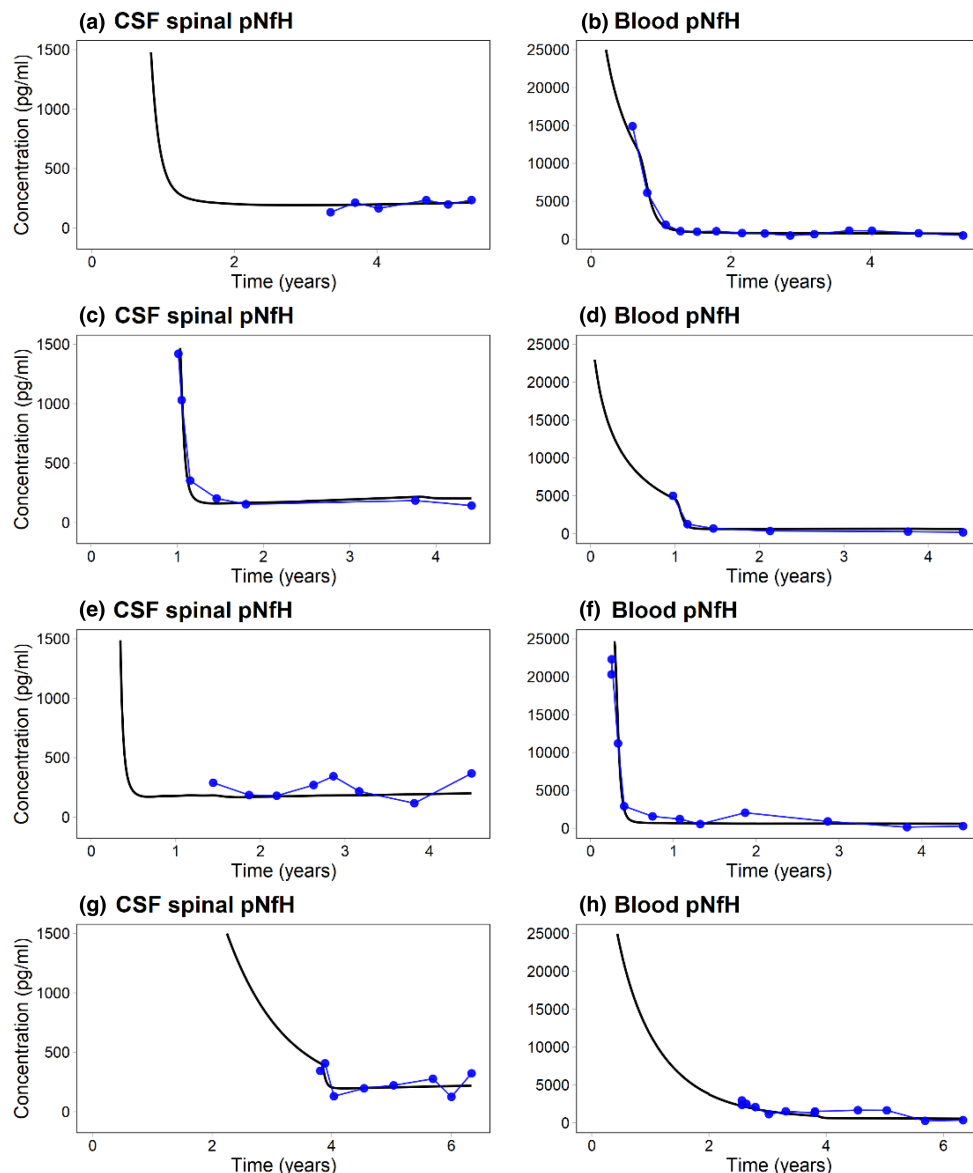
FIGURE 3 pNfH time series (blue dots and broken lines) in CSF (left) and blood (right) of four patients participating in the trial (represented by the pairs of panels: a and b, c and d, e and f, and g and h), chosen as representative of the overall individual fits compared with the corresponding time series as simulated by the model (black continuous line). The patients were enrolled in trials ENDEAR, EMBRACE, ENDEAR and CHERISH, respectively. CSF, cerebrospinal fluid; pNfH, phosphorylated neurofilament heavy subunit

direction of considering longitudinal growth population data[25] and modeling them in a mathematical way by introducing time-dependent volume changes and additional terms in the Nf ODEs. This was due to the necessity of simulating the prolonged time of observation of each subject, which reaches up to 5 years, thus requiring a punctual estimation of the real volume growth. The dynamics of the volume changes were derived by combining different data sources[16,17,21] to obtain age-dependent functions that represent the average growth of the volume in the population. This upgrade of the model is open to further improvements such as the use of percentile distributions or even individual body

indexes if the potential model applications will require a more refined level of detail.

The other important aspect incorporated in the model is a description of postnatal nervous system development, which is an extremely complex and poorly understood process. Nf concentration data in the different regions of the CNS are scarce,[26,27] and, to our knowledge, longitudinal studies are absent. For this reason, we modeled the Nf dynamics in CNS by relying on the change in the density of neuronal connections,[20] assuming the Nf concentration to be proportional to the neuronal density function and the leakage reaction r5 to be proportional to the derivative of the same function. Despite the numerous uncertainties,
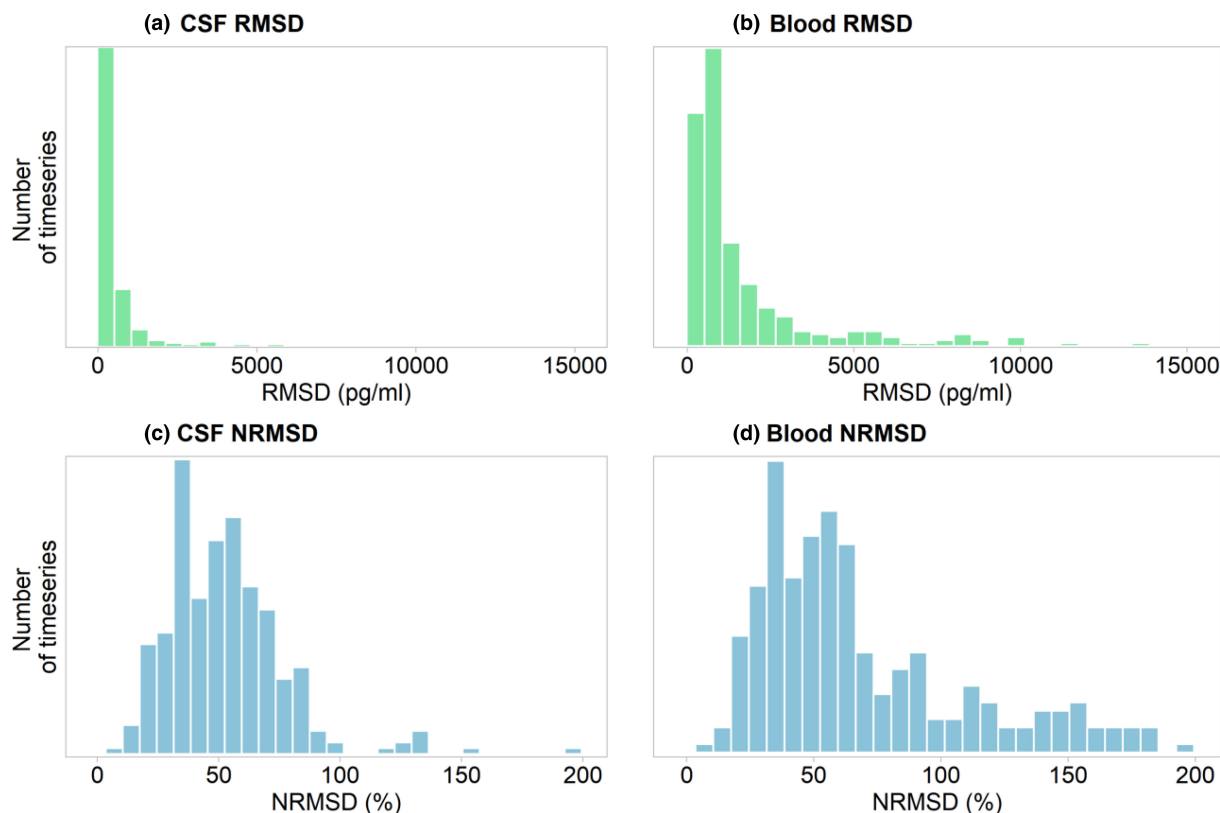
FIGURE 4 Histograms of the RMSDs between the simulated mean time series obtained by the individual fits of the data and the experimental time series in cerebrospinal fluid (CSF) (a) and blood (b). Histograms of the NRMSD of the same fits, as computed in Equation (1) in CSF (c) and blood (d). CSF, cerebrospinal fluid; NRMSD, normalized root mean square deviation; RMSD, root mean square deviation

these assumptions demonstrated to work reasonably well in fitting the pNfH levels of healthy subjects, leaving room for the possibility of further improving the description when new information becomes available. The much higher pNfH concentrations observed in most SMA patients with respect to healthy subjects indicates that the increased leakage due to SMA dominates over the physiological contribution and that uncertainties about the healthy scenario are not supposed to significantly affect the modeling results in the presence of the disease, especially for younger patients.

The higher pNfH concentrations observed in SMA patients have been captured by the additional flux from the PNS reflected by the reaction r14. The rate was modeled in a phenomenological way by considering the dependency of the pNfH level on age and abstracting from the details at the molecular level of how the disease produces the leakage increase. The in silico population built by fitting the data confirmed a posteriori the validity of the formulation of the new rates, working well in almost all cases. This is noteworthy, considering that the sample includes patients with heterogeneous age and disease severity. However, the reaction is purely phenomenological, and it does not shed any light on the mechanism underlying

the increased pNfH release from the nervous system. As reported in the Results section, the only situation where the in silico population seems to be less accurate is in newborns from the NURTURE trial (see Figure 2), for which simulated CSF levels seem to underestimate the average pNfH concentration and prevent a faithful reproducibility of the large intersubject variability toward higher Nf levels. We identify two potential causes to which we could ascribe this potential weakness of the model. The first is a possible permeability of the blood–brain barrier[28] during its maturation, which is not considered in our current model and would allow for a direct Nf transport between ISF and blood, with a consequent effect on the Nf levels also in the CSF. The second is a variation of the CSF turnover with age[29] that would potentially affect the reactions from r7 to r12. Future tests of these two hypotheses leave space for a refinement of the model in light of available clinical data of the treatment in the neonatal age.[12]

The parameter estimates computed for the untreated population constituted a reference to analyze those derived from the fit of the individual time series of treated patients. An analysis of the optimized parameter values indicates that the larger variability could be attributed to the estimate of the initial Nf concentrations. This is
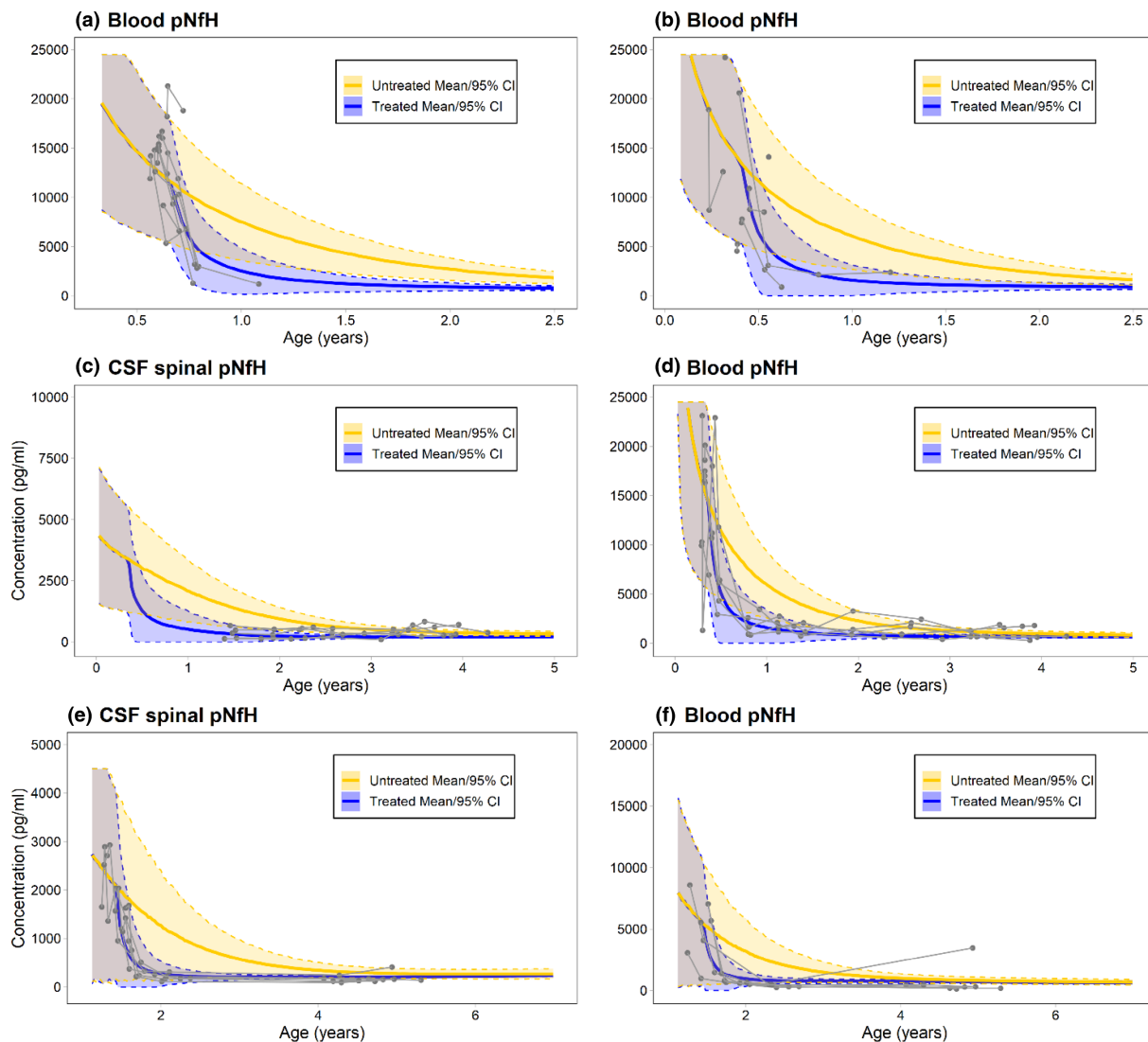
FIGURE 5 Model validations performed on four groups of treated patients. For two of them (a and b), only data in plasma are available, whereas the other two validation groups (c and d, e and f) also include data on CSF. Mean and 95% CI of the simulated untreated (yellow) and treated (blue) conditions are compared with the measured time series of the treated patients (gray dots and broken lines). Detailed information about the doses administered for each validation group is reported in Table S2. CI, confidence interval; CSF, cerebrospinal fluid; pNfH, phosphorylated neurofilament heavy subunit

reasonable, considering that for many patients the sampling in one or in both compartments started even months after the start of the treatment, adding unavoidable uncertainty to the fits.

Nusinersen acts on the synthesis of SMN, and thus the observed reduction of pNfH levels is a secondary effect. Our choice to model this mechanism of action was the inclusion of transit compartments[21] in the model. This allows for the direct inclusion of the individual drug time series computed from a pharmacokinetics (PK) model of nusinersen[18] and at the same time this introduces a delay and a smoothed effective leakage function to reproduce at best the pNfH time series. The individual fits confirmed that this approach is generally working, even if the age of the patients and the administered dosage were heterogeneous. Regarding this

observation, we investigated the presence of correlations between the optimized parameter estimates and the age of the patients, but we did not observe any, confirming that the model seems to work generally well at all ages. The selected PK model[18] is similar to another published model that describes the whole-body distribution of ASOs.[30] They share some similarity in the structure and connectivity of the main CNS compartments, and both are empirical in terms of parameter estimation, which is informed by the terminal tissue sampling in NHP studies. The nusinersen ASO PK model used in this work considers a long terminal elimination half-life in the CNS tissues and CSF (~4–6 months), which was also found to be consistent between NHPs and humans,[18] demonstrating suitability in predicting the time series of the total amount of the therapeutic ASO

calculated across the lumbar, thoracic, and cervical spinal cord segments.

The validation scenarios, considering homogeneous groups of patients with different ages and treatment protocols, confirm good model capabilities in predicting the average pNfH level decrease. This is particularly evident in the loading phase of treatment, where the decrease is particularly accentuated and the separation from the otherwise untreated condition is larger. In the longer runs of the treatment simulation, the shrinking CI band indicates that the model could be further refined to better capture the individual variability in later phases of the treatment.

The dose amounts used to estimate the treatment parameters were heterogeneous, although most patients received dosages correspondent to or not very far from the nusinersen 12-mg dose regimen, and the model worked reasonably well in the various cases. Despite this fact, it remains an open question if model predictions remain reliable for dosages very different from those considered in this work and, for this reason, additional work relying on clinical data considering higher doses[31] could be performed in future.

AUTHOR CONTRIBUTIONS

CONFLICT OF INTEREST

FUNDING INFORMATION

ORCID

Xiao Tong https://orcid.org/0000-0002-0405-6429
Luca Marchetti https://orcid.org/0000-0001-9043-7705

REFERENCES

1. Lunn MR, Wang CH. Spinal muscular atrophy. *The Lancet*. 2008;371(9630):2120-2133.
2. D'Amico A, Mercuri E, Tiziano FD, Bertini E. Spinal muscular atrophy. *Orphanet J Rare Dis*. 2011;6(1):1.
3. Lefebvre S, Burlet P, Liu Q, et al. Correlation between severity and SMN protein level in spinal muscular atrophy. *Nat Genet*. 1997;16(3):265-269.
4. Finkel RS, Mercuri E, Darras BT, et al. Nusinersen versus sham control in infantile-onset spinal muscular atrophy. *N Engl J Med*. 2017;377:1723-1732.
5. Gaiottino J, Norgren N, Dobson R, et al. Increased neurofilament light chain blood levels in neurodegenerative neurological diseases. *PloS One*. 2013;8(9):e75091.
6. Khalil MT, Teunissen CE, Otto M, et al. Neurofilaments as biomarkers in neurological disorders. *Nat Rev Neurol*. 2018;14(10):577-589.
7. Yuan A, Rao MV, Veeranna, Nixon RA. Neurofilaments and Neurofilament proteins in health and disease. *Cold Spring Harb Perspect Biol*. 2017;9(4):a018309.
8. Darras BT, Crawford TO, Finkel RS, et al. Neurofilament as a potential biomarker for spinal muscular atrophy. *Ann Clin Trans Neurol*. 2019;6(5):932-944.
9. Wurster CD, Steinacker P, Günther R, et al. Neurofilament light chain in serum of adolescent and adult SMA patients under treatment with nusinersen. *J Neurol*. 2020;267(1):36-44.
10. Paris A, Bora P, Parolo S, et al. An age-dependent mathematical model of neurofilament trafficking in healthy conditions. *CPT Pharmacometrics Syst Pharmacol*. 2022;11:447-457.
11. Castro D, Finkel RS, Farrar MA, et al. Nusinersen in infantile-onset spinal muscular atrophy: results from longer-term treatment from the open-label SHINE extension study (1640). *Neurology*. 2020;94(15):1640.
12. Darryl C, Bertini E, Swoboda KJ, Hwu WL, Crawford TO, Finkel RS. Nusinersen initiated in infants during the presymptomatic stage of spinal muscular atrophy: interim efficacy and safety results from the phase 2 NURTURE study. *Neuromuscul Disord*. 2019;29(11):842-856.
13. Acsadi G, Crawford TO, Müller-Felber W, Shieh PB, Richardson R, Natarajan N. Safety and efficacy of nusinersen in spinal muscular atrophy: the EMBRACE study. *Muscle Nerve*. 2021;63(5):668-677.
14. Finkel R, Kuntz N, Mercuri E, Chiriboga CA, Darras B, Topaloglu H. Efficacy and safety of nusinersen in infants with spinal muscular atrophy (SMA): final results from the phase 3 ENDEAR study. *Eur J Paediatr Neurol*. 2017;21:e14-e15.
15. Mercuri E, Darras BT, Chiriboga CA, et al. Nusinersen versus sham control in later-onset spinal muscular atrophy. *New England Journal of Medicine*. 2018;378(7):625-635.
16. Yang F, Xianping Tong D, McCarver G, Hines RN, Beard DA. Population-based analysis of methadone distribution and metabolism using an age-dependent physiologically based pharmacokinetic model. *J Pharmacokinet Pharmacodyn*. 2006;33(4):485-518.
17. CDC Clinical Grow Charts. 2017. Accessed November 22, 2022. https://www.cdc.gov/growthcharts/clinical_charts.htm.
18. Biliouris K, Gaitonde P, Yin W, et al. A semi-mechanistic population pharmacokinetic model of nusinersen: an antisense oligonucleotide for the treatment of spinal muscular atrophy. *CPT Pharmacometrics Syst Pharmacol*. 2018;7(9):581-592.
19. Huttenlocher PR, Dabholkar AS. Regional differences in synaptogenesis in human cerebral cortex. *J Comp Neurol*. 1997;387(2):167-178.
20. Petanjek Z, Judaš M, Šimić G, et al. Extraordinary neoteny of synaptic spines in the human prefrontal cortex. *Proc Natl Acad Sci*. 2011;108(32):13281-13286.
21. Sun Y-N, Jusko WJ. Transit compartments versus gamma distribution function to model signal transduction processes in pharmacodynamics. *J Pharm Sci*. 1998;87(6):732-737.
22. Wilke C, Pujol-Calderon F, Barro C, et al. Correlations between serum and CSF pNfH levels in ALS, FDT and controls:

a comparison of three analytical approaches. *Clin Chem Lab Med*. 2019;57(10):1556-1564.

23. Allen RJ, Rieger TR, Musante CJ. Efficient generation and selection of virtual populations in quantitative systems pharmacology models. *CPT Pharmacometrics Syst Pharmacol*. 2016;5(3):140-146.

24. Mahmood I. Dosing in children: a critical review of the pharmacokinetic allometric scaling and modelling approaches in paediatric drug development and clinical settings. *Clin Pharmacokinet*. 2014;53(4):327-346.

25. Nierop AF, Niklasson A, Holmgren A, Gelander L, Rosberg S, Albertsson-Wikland K. Modelling individual longitudinal human growth from fetal to adult life− QEPS I. *J Theor Biol*. 2016;406:143-165.

26. Ferrer-Alcón M, García-Sevilla JA, Jaquet PE, et al. Regulation of nonphosphorylated and phosphorylated forms of neurofilament proteins in the prefrontal cortex of human opioid addicts. *J Neurosci Res*. 2000;61(3):338-349.

27. Hashimoto R, Nakamura Y, Tsujio I, Tanimukai H, Kudo T, Takeda M. Quantitative analysis of neurofilament proteins in Alzheimer brain by enzyme linked immunosorbent assay system. *Psychiatry Clin Neurosci*. 1999;53(5):587-591.

28. Saunders NR, Liddelow SA, Dziegielewska KM. Barrier mechanisms in the developing brain. *Front Pharmacol*. 2012;29(3):46.

29. Wachi A, Kudo S, Sato K. Characteristics of cerebrospinal fluid circulation in infants as detected with MR velocity imaging. *Childs Nerv Syst*. 1995;11(4):227-230.

30. Monine M, Norris D, Wang Y, Nestorov I. A physiologically-based pharmacokinetic model to describe antisense oligonucleotide distribution after intrathecal administration. *J Pharmacokinet Pharmacodyn*. 2021;5:639-654.

31. Day JW, Pascual-Pascual SI, Finkel RS et al. Escalating Dose and Randomized, Controlled Study of Nusinersen in Participants With Spinal Muscular Atrophy (SMA); Study Design and Part A Data for the Phase 2/3 DEVOTE (232SM203) Study to Explore High Dose Nusinersen (2343). 2021.

SUPPORTING INFORMATION

Additional supporting information can be found online in the Supporting Information section at the end of this article.